

# Comprehensive Multimodal Imaging in Tuberous Sclerosis Complex: A Case Report

SANMEET GUMBER<sup>1</sup>, SHIVALI KASHIKAR<sup>2</sup>, PRATAP SINGH HANUMAN PARIHAR<sup>3</sup>, PALLAVI KAR<sup>4</sup>, ARINDAM GUPTA<sup>5</sup>

## ABSTRACT

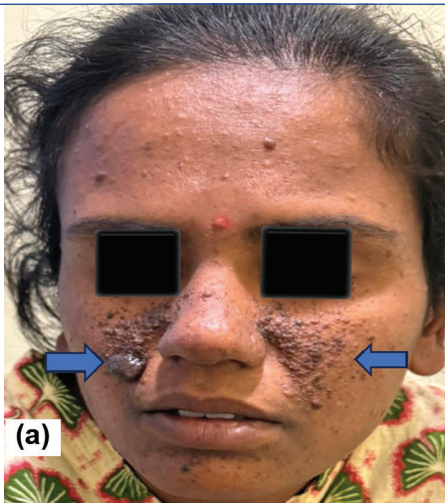
Tuberous Sclerosis Complex (TSC) is an autosomal dominant disorder caused by mutations in the TSC1 (hamartin) or TSC2 (tuberin) genes, affecting multiple organ systems. A 23-year-old female presented with cosmetic concerns due to malodorous facial plaques and oral papules. Clinical examination revealed characteristic skin manifestations such as facial angiofibromas and hypomelanotic macules. Magnetic Resonance Imaging (MRI) of the brain showed subependymal and subcortical tubers with radial bands, while abdominal ultrasound and Computed Tomography (CT) scans demonstrated bilateral renal angiomyolipomas and pulmonary cystic lesions, suggesting Lymphangioleiomyomatosis (LAM). TSC impacts both children and adults, with significant variability in clinical features, even within families. Early recognition of imaging findings such as radial migration lines and renal angiomyolipomas can significantly improve outcomes. Multimodal imaging is crucial in assessing disease severity and planning appropriate management.

**Keywords:** Hamartin and tuberin, mTOR signalling pathway, Neuropsychiatric disorders

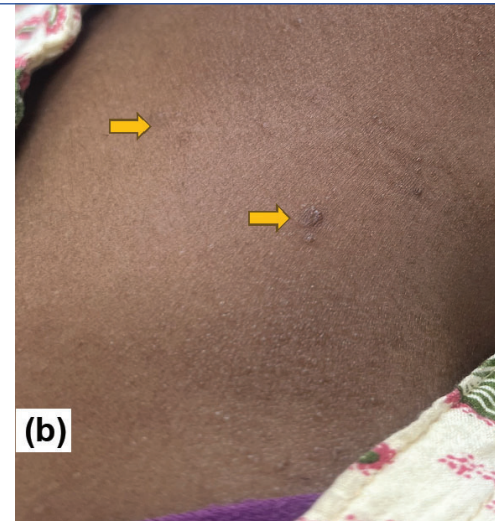
## CASE REPORT

A 23-year-old female patient came into the dermatology outpatient department with a complaint of malodorous plaques on her face and neck that had been there for two years, as well as papules in her mouth that had been there for five or six years. She was the child of a non-consanguineous union. There was a history of delayed developmental milestones, including late neck holding (achieved after five months), sitting without support (after 10 months), and delayed speech initiation, with first meaningful words spoken after three years of age. There was no familial history of TSC. There was no complaint of jerky movements, backache, hazy vision, abdominal pain, or urinary complaints.

Examinations of the patient's systemic and general physicals were normal. Several discrete to coalescent, dark brown to erythematous papules and plaques, some pedunculated lesions were found mostly across the central face [Table/Fig-1a], and during cutaneous examination, these findings suggested the presence of angiofibromas, also hypomelanotic macules on the neck [Table/Fig-1b], right forearm [Table/Fig-1c], and bilateral thigh region [Table/Fig-1d] were also present.



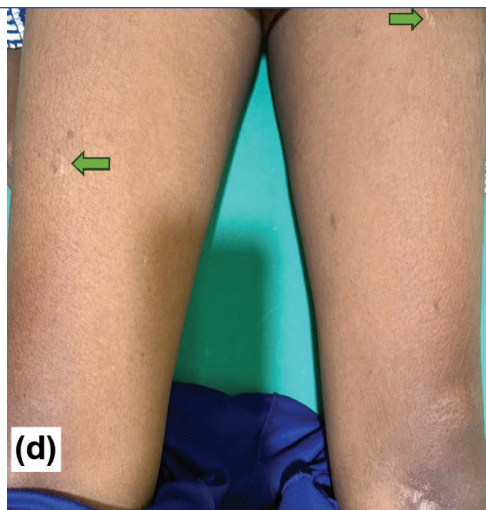
[Table/Fig-1a]: Numerous erythematous to hyperpigmented large and small angiofibromas over the face (blue arrow).



[Table/Fig-1b]: Hypomelanotic macules on the neck (yellow arrow).

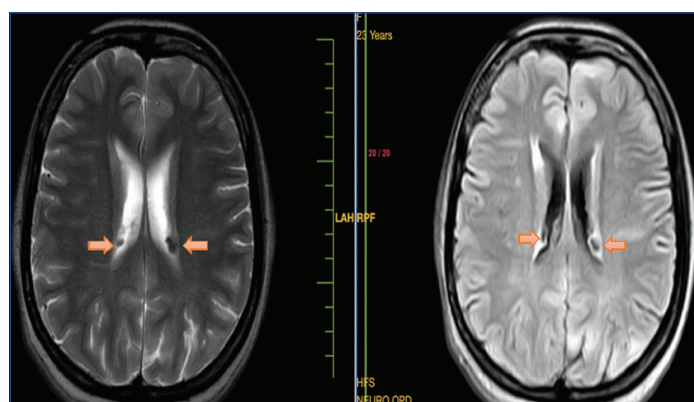


[Table/Fig-1c]: Hypomelanotic macules on the right forearm (orange arrow).

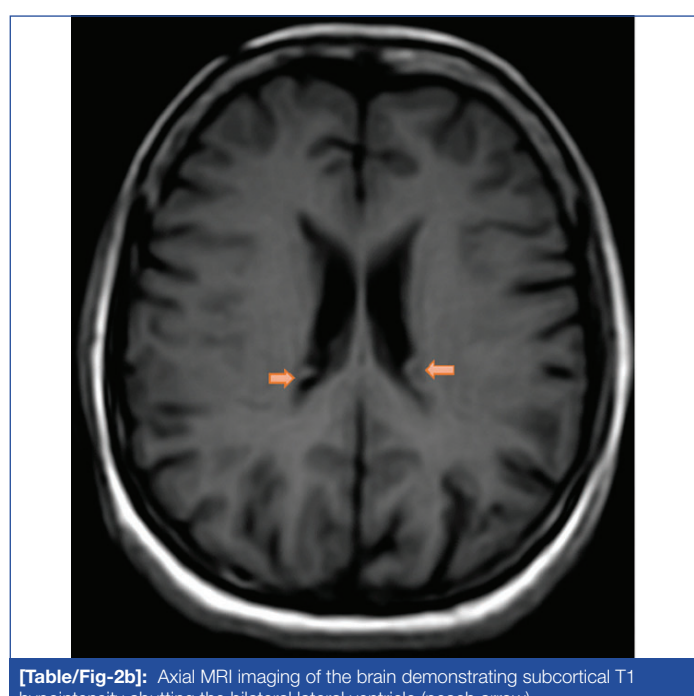


[Table/Fig-1d]: Hypomelanotic macules on bilateral thighs (green arrow).

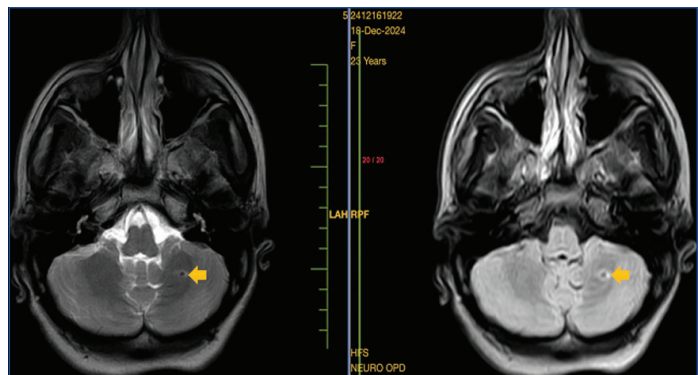
Additionally, axial sections of MRI showed multiple subcortical and subependymal T2/FLAIR hyperintense and T1 hypointense lesions abutting the bilateral lateral ventricles ([Table/Fig-2], respectively), left cerebellar hemisphere ([Table/Fig-3a,b], respectively), and a similar lesion abutting the occipital horn of the left lateral ventricle ([Table/Fig-4a,b], respectively), which appears to be adjacent to it. All the lesions show blooming on Susceptibility Weighted Imaging (SWI) and seem bright on phase images that depict calcified tubers on axial MRI sections of the brain [Table/Fig-5a-c].



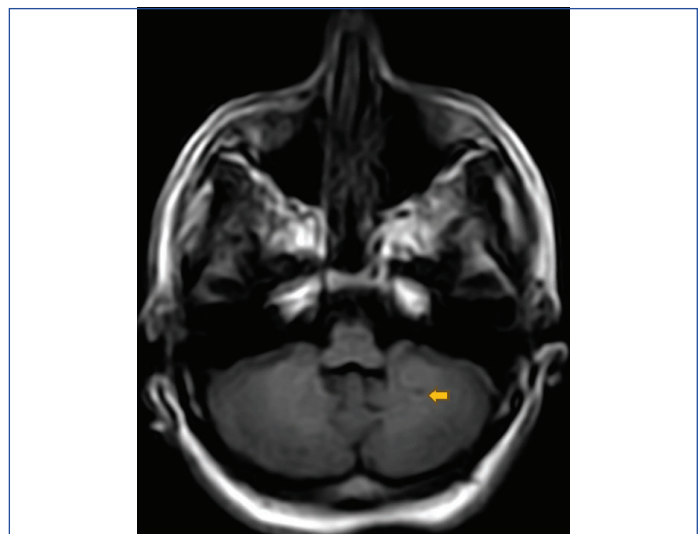
[Table/Fig-2a]: Axial MRI imaging of the brain demonstrating subcortical T2/FLAIR hyperintensity abutting the bilateral lateral ventricle (peach arrow).



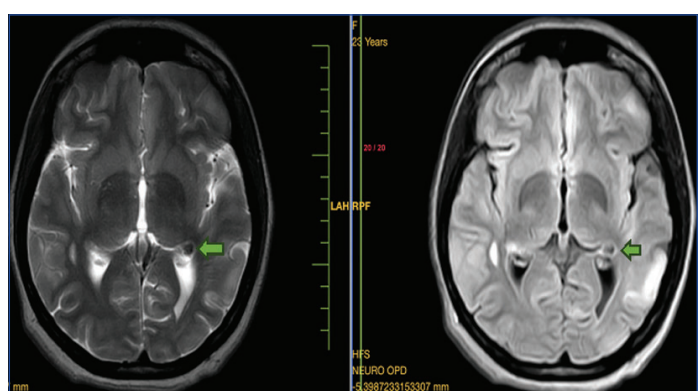
[Table/Fig-2b]: Axial MRI imaging of the brain demonstrating subcortical T1 hypointensity abutting the bilateral lateral ventricle (peach arrow).



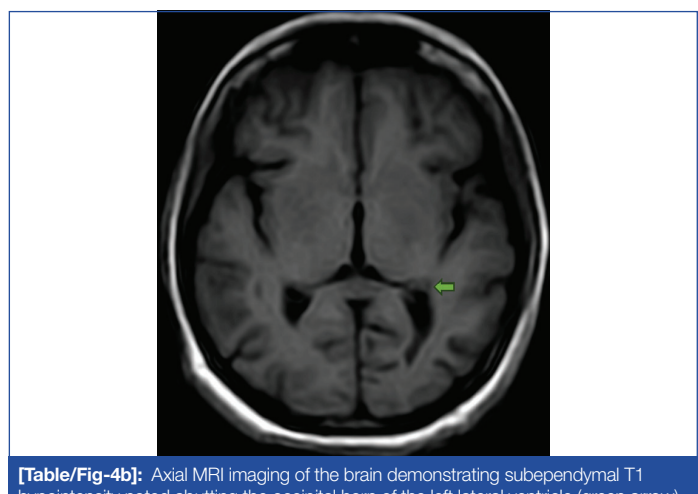
[Table/Fig-3a]: Axial MRI imaging of the brain demonstrating T2/FLAIR hyperintensity noted in the left cerebellar hemisphere (yellow area).



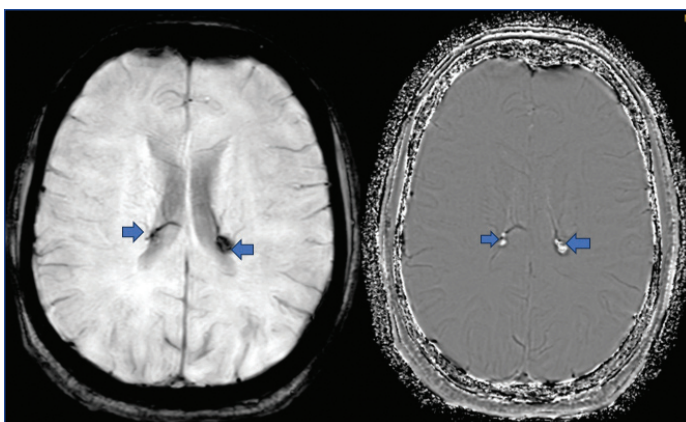
[Table/Fig-3b]: Axial MRI imaging of the brain demonstrating T1 hypointensity noted in the left cerebellar hemisphere (yellow arrow).



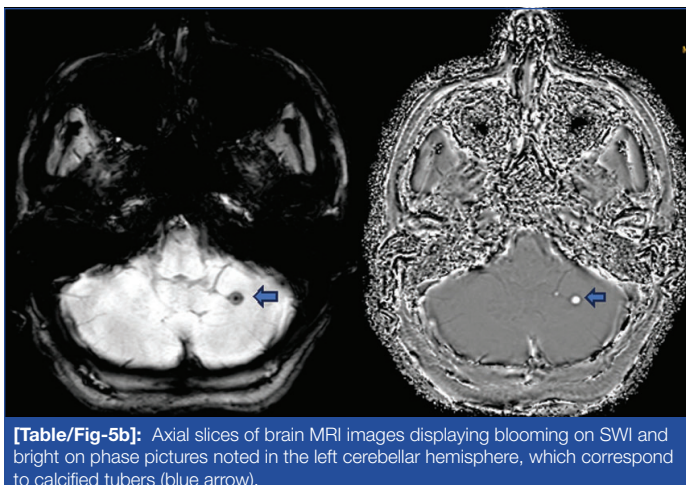
[Table/Fig-4a]: Axial MRI imaging of the brain demonstrating subependymal T2/FLAIR hyperintensity noted abutting the occipital horn of left lateral ventricle (green arrow).



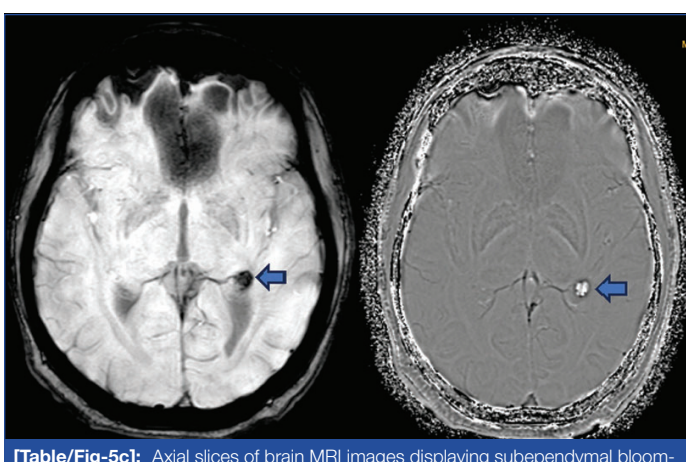
[Table/Fig-4b]: Axial MRI imaging of the brain demonstrating subependymal T1 hypointensity noted abutting the occipital horn of the left lateral ventricle (green arrow).



**[Table/Fig-5a]:** Axial slices of brain MRI images displaying blooming on SWI and bright on phase pictures abutting bilateral lateral ventricles, which correspond to calcified subcortical tubers (blue arrow).



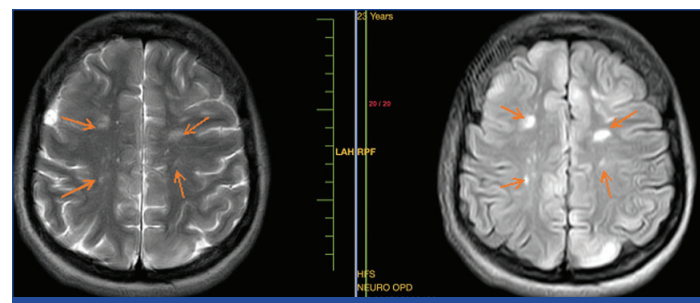
**[Table/Fig-5b]:** Axial slices of brain MRI images displaying blooming on SWI and bright on phase pictures noted in the left cerebellar hemisphere, which correspond to calcified tubers (blue arrow).



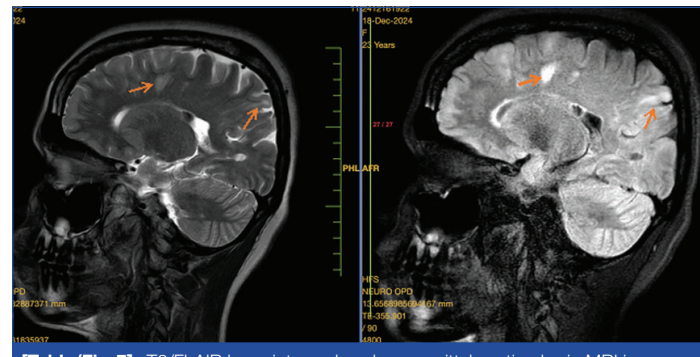
**[Table/Fig-5c]:** Axial slices of brain MRI images displaying subependymal blooming on SWI and bright on phase pictures abutting the occipital horn of the left lateral ventricle, which correspond to calcified subependymal tubers (blue arrow).

Axial sections of MRI also revealed T2/FLAIR white matter hyperintensities in bilateral fronto-parietal lobes [Table/Fig-6], and sagittal sections of MRI brain reveal T2/FLAIR hyperintense linear bands radiating from periventricular white matter to the subcortical white matter in bilateral frontal and parietal lobes, representing radial bands [Table/Fig-7].

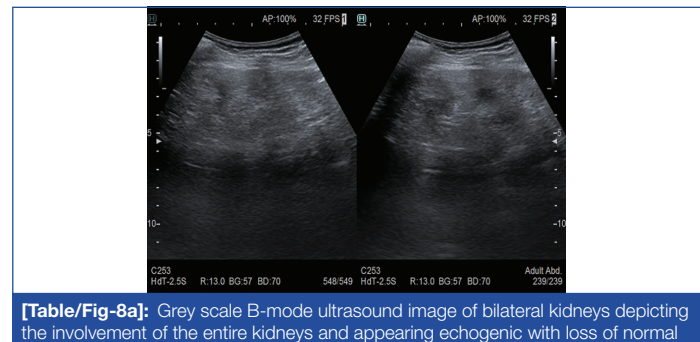
After obtaining the mother's consent, we conducted an abdominal ultrasound that showed mild enlargement of bilateral kidneys with heterogeneous echotexture and non-visualisation of cortico-medullary junction due to multiple well-delineated, rounded hyperechoic masses in bilateral kidneys representing angiomyolipomas [Table/Fig-8a,b]. Based on the knowledge of clinical history, skin lesions, and neurological findings of MRI strong suspicion of TS was made. There was no evidence of bilateral hydronephrosis. Additionally, several small hyperechoic lesions that resembled haemangiomas were observed in both liver lobes [Table/Fig-9].



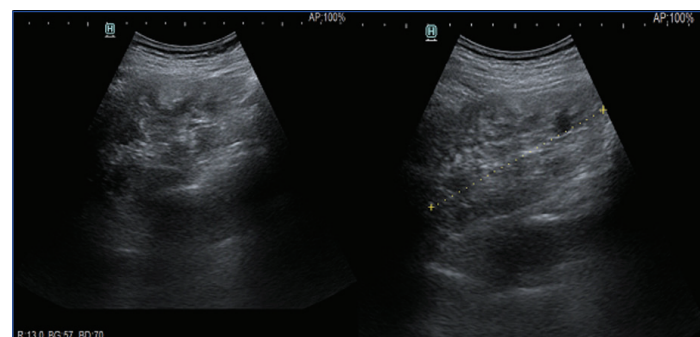
**[Table/Fig-6]:** Axial portions of brain MRI images demonstrating T2/FLAIR hyperintensities in bilateral fronto-parietal lobes (Orange arrows).



**[Table/Fig-7]:** T2/FLAIR hyperintense bands on sagittal section brain MRI images are observed to radiate from periventricular white matter to subcortical white matter in bilateral fronto-parietal lobes, signifying radial bands (orange arrows).



**[Table/Fig-8a]:** Grey scale B-mode ultrasound image of bilateral kidneys depicting the involvement of the entire kidneys and appearing echogenic with loss of normal cortico-medullary junction.

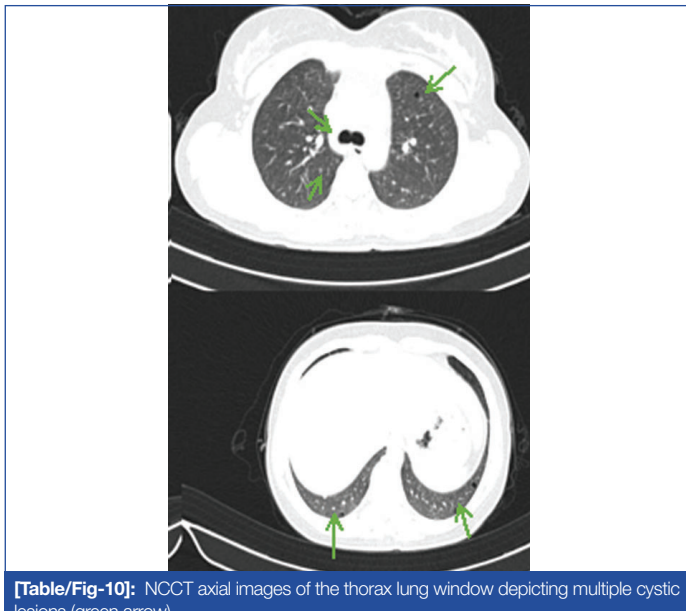


**[Table/Fig-8b]:** Grey scale B-mode ultrasound image of bilateral kidneys depicting multiple hyperechoic lesions involving the entire parenchyma of the kidneys s/o angiomyolipomas.

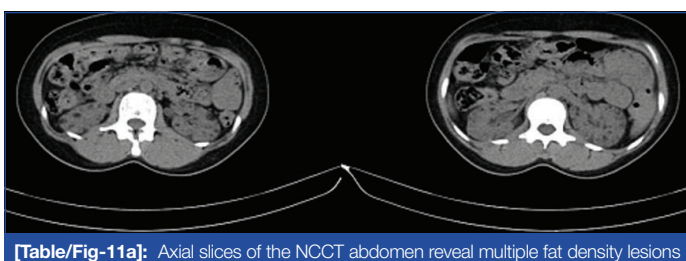


**[Table/Fig-9]:** Grey scale B-mode ultrasound image depicting a few well-defined hyperechoic lesions in the bilateral lobes of the liver representing haemangioma (green arrow).

To ascertain the multisystemic form of the disease, we advised the patient to get a Computed Tomography (CT) scan of the thorax and abdomen. On axial pictures of the thorax lung window, the patient's Non-Contrast Computed Tomography (NCCT) thorax showed several cystic lesions in the posterior segments of both lower lobes of the lungs, the anterior segment of the left upper lobe, and the apical segment of the right upper lobe [Table/Fig-10]. Axial [Table/Fig-11a] and coronal [Table/Fig-11b] slices of the NCCT abdomen revealed multiple fat-density lesions dispersed throughout the bilateral renal parenchyma.



**[Table/Fig-10]:** NCCT axial images of the thorax lung window depicting multiple cystic lesions (green arrow).



**[Table/Fig-11a]:** Axial slices of the NCCT abdomen reveal multiple fat density lesions dispersed throughout the bilateral renal parenchyma s/o multiple angiomyolipomas.



**[Table/Fig-11b]:** Coronal slice of the NCCT abdomen reveals multiple fat density lesions dispersed throughout the bilateral renal parenchyma s/o multiple angiomyolipomas.

After completing imaging, the patient was counselled in detail about the multisystemic nature of TSC. For her cosmetic concerns, dermatological management was planned, including consideration of laser ablation for facial angiofibromas and topical sirolimus. Neurology

consultation was advised for baseline Electroencephalography (EEG) and ongoing neuropsychiatric evaluation.

Additionally, she was enrolled in a multidisciplinary follow-up programme involving dermatology, neurology, nephrology, and pulmonology. Periodic imaging, renal function tests, and mTOR inhibitor therapy were discussed as part of long-term management to address systemic involvement and prevent complications.

## DISCUSSION

The TSC is an autosomal dominant disorder primarily marked by facial angiofibromas, persistent epilepsy, and intellectual disability [1]. It also presents with retinal hamartomas, renal angiomyolipomas, and hypopigmented skin lesions [2-4]. Neuroimaging reveals subependymal calcified nodules on CT and radial bands with abnormal T1/T2 signals on MRI. Renal angiomyolipomas occur in 55-75% of cases and risk haemorrhage when >3 cm due to associated aneurysms [2-4]. LAM, mostly affecting women, is marked by cystic lung changes and abnormal smooth muscle proliferation [5]. Over 80% of patients have cortical tubers, closely associated with epilepsy, cognitive deficits, and autism, representing cortical developmental anomalies [6-8]. Seizures often resist antiepileptic therapy [5], and surgical excision of tubers, which are typically epileptogenic foci, may be required for refractory epilepsy [9,10].

It is a genetic disorder characterised by benign tumour formation across multiple organs due to dysregulation in cell growth and proliferation. The disorder stems from inactivating mutations in either the TSC1 gene (encoding hamartin) or the TSC2 gene (encoding tuberin) [11]. These proteins, in association with TBC1D7, form a heterotrimeric TSC complex that negatively regulates the mTORC1 pathway-a critical intracellular signalling cascade involved in cellular metabolism, protein synthesis, and growth [12]. Loss of function of this complex leads to constitutive activation of mTORC1, resulting in uncontrolled cellular proliferation and hamartoma formation in organs such as the brain, kidneys, heart, lungs, and skin [12,13].

Approximately 70% of TSC cases are caused by TSC2 mutations, while TSC1 accounts for 20%; the remainder involves non-coding regions or mosaicism [11]. TSC2 mutations tend to present with more severe phenotypes due to their larger deletions and rearrangements [12]. This genotypic-phenotypic variability contributes significantly to the clinical heterogeneity observed in TSC, making diagnosis complex and often delayed.

Diagnosis of TSC is complicated by variable symptom onset, mild early signs, and the possibility of non-classical presentations. For instance, early dermatologic signs such as hypopigmented macules may be overlooked, while neurological symptoms like seizures are often misattributed to more common etiologies [14]. Additionally, radiologic findings like cortical tubers, Subependymal Nodules (SENs), and Subependymal Giant Cell Astrocytomas (SEGA), are characteristic of the diagnosis, but sometimes it may be mistaken for other lesions [15].

The 2012 International TSC Consensus Conference defined revised diagnostic criteria, including clinical features (e.g., facial angiofibromas, renal angiomyolipomas, SENs) and genetic testing [16]. However, genetic confirmation, although definitive, is not always accessible or affordable in all regions, further delaying diagnosis [16].

In a case reported by Dedushi K et al., two paediatric patients were referred for recurrent seizures and behavioural disturbances [12]. Dermatological examination revealed hypomelanotic macules and facial angiofibromas. MRI brain showed characteristic radial migration lines and SENs, while abdominal ultrasound revealed renal angiomyolipomas. Genetic analysis further supported the diagnosis, despite the absence of a family history, underscoring the role of imaging and multidisciplinary evaluation in early diagnosis.

Li Y et al., described a five-year-old male presenting with speech delay, intellectual disability, and cardiac murmur [13].

Echocardiography identified multiple cardiac rhabdomyomas. MRI brain showed cortical tubers, SENs, and white matter abnormalities. The diagnosis of TSC was genetically confirmed with a TSC1 mutation. Early diagnosis in this case enabled prompt neurological and nephrological surveillance, preventing complications from renal angiomyolipoma identified later during follow-up.

Additionally, a case presented by Bhinder KK and Aslam S involved a young adult female who reported progressive breathlessness and multiple facial lesions [11]. High-resolution CT thorax revealed diffuse cystic lung changes consistent with pulmonary LAM. MRI brain showed multiple subependymal calcified nodules, and abdominal imaging confirmed bilateral renal angiomyolipomas. Genetic studies were supportive of the TSC2 mutation. This case highlighted the adult-onset manifestations of TSC, particularly pulmonary involvement, which is often under-recognised.

These reports demonstrate the diverse and sometimes deceptive presentations of TSC. They reaffirm the importance of integrating clinical history, detailed dermatologic and neurologic examination, multimodal imaging, and genetic testing to reach an accurate and timely diagnosis, especially in cases where the classical triad is incomplete or atypical symptoms predominate.

Given the multisystem nature of TSC and the lifelong risk of progressive organ involvement, early and periodic screening is essential. The following strategies are recommended:

- Neuroimaging (MRI of the brain) should be performed at diagnosis and repeated periodically to assess cortical tubers, SENs, and the development of SEGA [14,16].
- Echocardiography in infants and children to detect cardiac rhabdomyomas, often presenting antenatally or within the first year of life [14].
- Renal imaging (ultrasound or MRI) starting in infancy to monitor for angiomyolipomas, cysts, and potential malignancy [13].
- Pulmonary CT in adolescent and adult females to evaluate for LAM, especially if respiratory symptoms arise [11].
- Genetic testing should be performed when clinical suspicion is high- even in the absence of full criteria- as it can provide a definitive diagnosis and guide family counseling [16].

Early identification of imaging signs such as radial migration lines, white matter lesions, and SEGA growth is vital to prevent complications like hydrocephalus or intractable epilepsy [13]. With growing understanding of TSC pathogenesis, mTOR inhibitors (e.g., everolimus) now provide targeted therapy for several manifestations, including SEGA, renal AMLs, and refractory epilepsy, underscoring the need for early diagnosis and systemic evaluation [12].

## CONCLUSION(S)

The TSC is a multisystem disorder that manifests in a variety of imaging as well as clinical characteristics. Better imaging and testing techniques have raised TSC frequency estimates, allowing for the identification of people with milder symptoms. Early diagnosis, treatment, and better results can be achieved by identifying particular radiologic features.

## REFERENCES

- [1] Tsang SH, Sharma T. Tuberous sclerosis. *Adv Exp Med Biol.* 2018;1085:205-07.
- [2] Dabora SL, Jozwiak S, Franz DN, Roberts PS, Nieto A, Chung J, et al. Mutational analysis in a cohort of 224 tuberous sclerosis patients indicates increased severity of TSC2, compared with TSC1, disease in multiple organs. *Am J Hum Genet.* 2001;68:64-80.
- [3] Ewalt DH, Shefield E, Sparagana SP, Delgado MR, Roach ES. Renal lesion growth in children with tuberous sclerosis complex. *J Urol.* 1998;160:141-45.
- [4] Ryu JH, Moss J, Beck GJ, Lee JC, Brown KK, Chapman JT, et al. The NHLBI lymphangiomyomatosis registry: Characteristics of 230 patients at enrollment. *Am J Respir Crit Care Med.* 2006;173:105-11.
- [5] Thiele EA. Managing epilepsy in tuberous sclerosis complex. *J Child Neurol.* 2004;19:680-86.
- [6] Goodman M, Lamm SH, Engel A, Shepherd CW, Houser OW, Gomez MR. Cortical tuber count: A biomarker indicating neurologic severity of tuberous sclerosis complex. *J Child Neurol.* 1997;12(2):85-90. DOI: 10.1177/088307389701200203. PMID: 9075016.
- [7] Mizuguchi M, Takashima S. Neuropathology of tuberous sclerosis. *Brain Dev.* 2001;23(7):508-15. DOI: 10.1016/s0387-7604(01)00304-7. PMID: 11701246.
- [8] Park SH, Pepkowitz SH, Kerfoot C, De Rosa MJ, Poukens V, Wienecke R, et al. Tuberous sclerosis in a 20-week gestation fetus: Immunohistochemical study. *Acta Neuropathol.* 1997;94(2):180-86. DOI: 10.1007/s004010050691. PMID: 9255394.
- [9] Koh S, Jayakar P, Dunoyer C, Whiting SE, Resnick TJ, Alvarez LA, et al. Epilepsy surgery in children with tuberous sclerosis complex: Presurgical evaluation and outcome. *Epilepsia.* 2000;41:1206-13.
- [10] Weiner HL. Tuberous sclerosis and multiple tubers: Localizing the epileptogenic zone. *Epilepsia.* 2004;45:Suppl 4:41-42.
- [11] Bhinder KK, Aslam S. Radiological road map to tuberous sclerosis complex (TSC) - pictorial review. *Pak J Radiol.* 2023;33(1):28-39.
- [12] Dedush K, Hyseni F, Musa J, Saliaj K, Vokshi V, Guy A, et al. The importance of imaging in Tuberous Sclerosis Complex (TSC) in children: Two cases. *Radiol Case Rep.* 2022;17(1):399-403. Available from: <https://doi.org/10.1016/j.radr.2021.11.007>.
- [13] Li Y, Si Z, Zhao W, Xie C, Zhang X, Liu J, et al. Tuberous sclerosis complex: A case report and literature review. *Ital J Paediatr.* 2023;49:116. Available from: <https://doi.org/10.1186/s13052-023-01490-z>.
- [14] Curatolo P, Bombardieri R, Jozwiak S. Tuberous sclerosis. *Lancet.* 2008;372(9639):657-68. DOI: 10.1016/S0140-6736(08)61279-9. PMID: 18722871.
- [15] Northrup H, Koenig MK, Pearson DA, et al. Tuberous sclerosis complex. 1999 Jul 13 [Updated 2024 Aug 1]. In: Adam MP, Feldman J, Mirzaa GM, et al., editors. *GeneReviews® [Internet].* Seattle (WA): University of Washington, Seattle; 1993-2025. Available from: <https://www.ncbi.nlm.nih.gov/books/NBK1220/>.
- [16] Northrup H, Krueger DA. Tuberous sclerosis complex diagnostic criteria update: Recommendations of the 2012 International Tuberous Sclerosis Complex Consensus Conference. *Pediatr Neurol.* 2013;49(4):243-54. Available from: <https://doi.org/10.1016/j.pediatrneurool.2013.08.001>.

### PARTICULARS OF CONTRIBUTORS:

1. Junior Resident, Department of Radiology, Jawaharlal Nehru Medical College, DMIHER, Wardha, Maharashtra, India.
2. Professor, Department of Radiology, Jawaharlal Nehru Medical College, DMIHER, Wardha, Maharashtra, India.
3. Professor and Head, Department of Radiology, Jawaharlal Nehru Medical College, DMIHER, Wardha, Maharashtra, India.
4. Assistant Professor, Department of Radiology, Jawaharlal Nehru Medical College, DMIHER, Wardha, Maharashtra, India.
5. Junior Resident, Department of Radiology, Jawaharlal Nehru Medical College, DMIHER, Wardha, Maharashtra, India.

### NAME, ADDRESS, E-MAIL ID OF THE CORRESPONDING AUTHOR:

Dr. Sanmeet Gumber,  
Adarsh Colony, Near Old High Court Lane, Bilaspur-495001, Chhattisgarh, India.  
E-mail: sanmeetgumbersg@gmail.com

### AUTHOR DECLARATION:

- Financial or Other Competing Interests: None
- Was informed consent obtained from the subjects involved in the study? Yes
- For any images presented appropriate consent has been obtained from the subjects. Yes

### PLAGIARISM CHECKING METHODS:

- Plagiarism X-checker: Feb 24, 2025
- Manual Googling: Sep 29, 2025
- iThenticate Software: Oct 01, 2025 (6%)

### ETYMOLOGY:

Author Origin

### EMENDATIONS:

8

Date of Submission: **Feb 21, 2025**  
Date of Peer Review: **May 16, 2025**  
Date of Acceptance: **Oct 03, 2025**  
Date of Publishing: **Dec 01, 2025**